Journal of Statistical Physics, Vol. 62, Nos. 5/6, 1991

Field-Induced Anisotropy in Concentrated Systems of Rigid Particles and Macromolecules

Gerald G. Fuller,[1] Kaye Smith,[1] and Wesley R. Burghardt[1]

Received February 10, 1990; final June 27, 1990

This paper presents experimental results on the use of spectroscopic optical polarimetry to study structure in dense systems of rigid particles and rigid polymer liquid crystals. These measurements probe microstructural anisotropy induced by the application of electric fields in the case of dense suspensions of rigid spheres, or flow fields in the case of polymer liquid crystals. It is demonstrated that conservative linear dichroism can measure moments of the particle pair distribution function in dense suspensions. In liquid crystals, the dichroism is a result of field-induced anisotropy in the defect structure of the material.

KEY WORDS: Concentrated suspensions; suspensions; liquid crystals; polymer liquid crystals; electric field orientation; hydrodynamic orientation; dichroism; polarimetry.

1. INTRODUCTION

Structure in concentrated systems will necessarily involve length scales that are intermediate between the constituent particles or macromolecules and the sample as a whole. Gaining an understanding of the connection between the microstructure and bulk material properties requires measurements of appropriate aspects of the structure. Due to the length scales that are involved in most complex, concentrated liquids, optical methods are often the obvious choice to accomplish such measurements. This paper is concerned with the application of high-speed polarimetry to probe structural anisotropy in two applications: (1) electric field induced structure in dense suspensions of colloidal hard spheres, and (2) the fluid dynamics of polymer liquid crystals.

[1] Department of Chemical Engineering, Stanford University, Stanford, California 94305-5025.

0022-4715/91/0300-1025$06.50/0

These are both examples of systems with structure at intermediate length scales. In dense suspensions, bulk properties are controlled by the spatial positions of the centers of mass of the particles. This is described through the pair distribution function $g(\mathbf{r})$.[1,2] This function prescribes the probability of finding a particle at a position $\mathbf{r}$ from the center of a test particle, normalized by the number density of particles. Application of a field (hydrodynamic, electric, or magnetic) can distort this function, leading to structural anisotropy.

In polymer liquid crystals, structure can be present over a wide range of length scales. At the length scale of a single macromolecule, orientational coupling induces alignment of the chains according to any number of patterns (simple nematic, cholesteric, and smectic).[3] On a larger length scale are fluctuations in orientation that are coupled to the strength of elastic forces (bending, splay, and twist modes). Existing at still larger length scales are defects in the director field in the form of disclination lines.[4] These are generally on the order of 1 μm in size. Finally, larger textures can occur in the form of banded structures spanning distances of 10–100 μm. It is unclear what roles these different levels of structure play in the bulk properties (optical or mechanical) of liquid crystals, and microstructural measurements over various length scales are required to establish structure–property relationships.

2. THE REFRACTIVE INDEX TENSOR

Light scattered from a liquid will contain information about the conformation of the constituent scattering elements. The angular dependence of the scattered light, as well as its polarization properties, can be used to infer the structure and dynamics of the sample. Measurement of the angular distribution of scattered light intensity can yield the Fourier transform of the pair distribution function. This paper, however, is concerned with measurement of the polarization of the transmitted light. This measurement is sensitive to the refractive index tensor of the sample and produces *moments* of the pair distribution function.

The refractive index tensor $\mathbf{n} = \mathbf{n}' - i\mathbf{n}''$ controls the propagation of the electric vector $\mathbf{E} = \mathbf{A}e^{i\sigma}$ in a material. The real part of $\mathbf{n}$ induces shifts in the phase of $\mathbf{E}$, and the imaginary part is linked to attenuation processes (absorption or scattering). Scattering of light can both shift its phase and attenuate its amplitude. If the scattering elements are anisotropic and oriented, the scattering will become polarization dependent and the tensors $\mathbf{n}'$ and $\mathbf{n}''$ will become anisotropic. Two quantities, the birefringence $\Delta n'$ and the dichroism $\Delta n''$, will arise and are defined as the differences in the principal eigenvalues of $\mathbf{n}'$ and $\mathbf{n}''$ in the plane normal to the direction of

light propagation. A recent review article by Fuller[5] discusses the relationship of the macroscopic refractive index tensor to microstructural properties in a variety of materials.

Anisotropy in the refractive index tensor can also arise due to intrinsic effects, in addition to the scattering or form contributions mentioned above. Oriented macromolecules, for example, will produce birefringence due to intrinsic anisotropy in the polarizability and this will occur at any wavelength. Intrinsic dichroism, on the other hand, will only arise at wavelengths where oriented components absorb light. Experiments performed away from absorbing regions, therefore, can eliminate intrinsic dichroism effects so that only scattering or form dichroism will be present. This is not true of birefringence, where it is generally very difficult to separate intrinsic and form contributions. The system of hard, colloidal spheres that is the subject of one of the examples discussed here is an exception. In such a suspension, there is no intrinsic source of anisotropy in the polarizability. Anisotropy only occurs as a result of distortion of the spatial positions of the centers of mass of the spheres. Conversely, the polymer liquid crystal example presents a system where both intrinsic and form birefringence will occur.

There have been very few theoretical treatments to predict form birefringence and dichroism. The recent theory of Onuki and Doi,[6] originally developed for deformed polymer chains, and recently extended for the case of hard-sphere suspensions by Wagner *et al.*,[1] is the most appropriate description for the two problems presented here. By solving the Maxwell field equations in the limit of small fluctuations in number density, Onuki and Doi were able to derive a relation between fluctuations in the number concentration of scattering elements and the macroscopic dielectric tensor. Anisotropies in this tensor determine the conservative linear dichroism and birefringence of the material. The basic result is

$$\boldsymbol{\varepsilon} = -\frac{\varepsilon_0 A}{(2\pi)^3}\left(\frac{4\pi a^3}{3}\right)^2 \int d\mathbf{q}\, C(\mathbf{k}-\mathbf{q})\left(\frac{\mathbf{qq}-k^2\boldsymbol{\delta}}{q^2-k^2}\right) \tag{1}$$

where

$$C(\mathbf{q}) = \int d\mathbf{r}\, e^{-i\mathbf{qr}}\langle \delta\varrho(0)\,\varrho(\mathbf{r})\rangle \tag{2}$$

$$A = \left(\frac{1}{\varepsilon_0}\frac{d\varepsilon_0}{d\phi}\right)^2 \tag{3}$$

In Eq. (2), $\delta\varrho(\mathbf{r})$ is the local fluctuation in the number density of the scattering elements, ε_0 is the mean dielectric constant of the fluid, and ϕ is the

volume fraction of the scattering elements. The vector **k** in Eq. (1) is the wave vector of the light and a is the radius of a scattering element. It should be noted the function $C(\mathbf{q})$ is the Fourier transform pair function of $g(\mathbf{r})$.

From a calculation of the dielectric tensor, the refractive index tensor **n**, which is the physically observable quantity in the experiments described below, is determined. The relationship between this two tensors is simply $\mathbf{n} = \sqrt{\boldsymbol{\varepsilon}}$. Recently, Adriani and Gast[2] have applied this theory to calculate the optical anisotropy of a system of rigid spheres subject to the combined effects of electric and shear fields.

3. POLARIMETRY APPARATUS

Techniques to rapidly measure $\mathbf{n}'$ and $\mathbf{n}''$ simultaneously in time have been developed in our laboratory using high-speed polarization modulation techniques. The apparatus used in the present study is shown in Fig. 1 and has been described in detail in ref. 7. Only dichroism measurements are reported here.

The light source consists of a xenon arc lamp and monochromator combination that provides radiation throughout the visible spectrum. The light is then polarized using a quartz polarizer and sent through a high-speed rotary polarization modulator. This is simply a monochromatic half-wave plate mounted in a high-speed turbine supported by an air bearing. The light leaving this unit is linearly polarized and spinning at 10 kHz. The light is then passed through the sample (either an electric field cell in the case of the suspensions, or a parallel plate flow cell for the polymer liquid crystals).

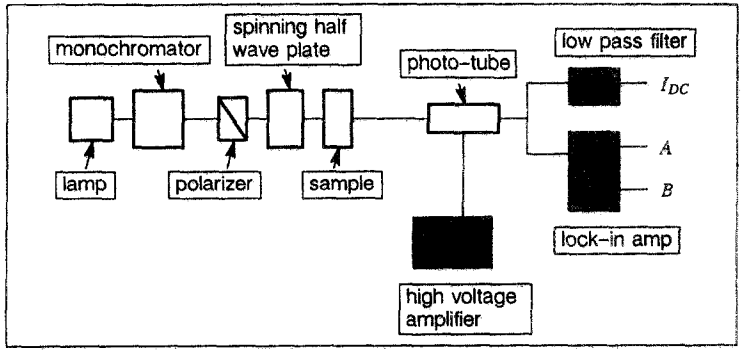

Fig. 1. Experimental arrangement used for the spectroscopic dichroism measurements. The outputs generated by the lock-in amplifier are $I_{DC} = I_0$, $A = -\sin 2\theta \tanh \delta''$, and $B = -\cos 2\theta \tanh \delta''$.

A photomultiplier tube measures the light intensity. This intensity is of the form

$$I = I_0(1 - \sin 2\theta \tanh \delta'' \sin 4\omega t - \cos 2\theta \tanh \delta'' \cos 4\omega t) \quad (4)$$

where ω is the angular velocity of the half-wave plate and I_0 is the incident intensity.

This signal is demodulated using a dual-phase lock-in amplifier to determine the extinction $\delta'' = 2\pi \Delta n'' d/\lambda$ and sample orientation angle θ measured with respect to the incident polarizer. Here d is the sample thickness and λ is the wavelength of the light. In the experiments conducted here, the electric and flow fields are oriented either parallel or othogonal to the initial polarizer. Because of this symmetry, $\theta = 0$ or $\pi/2$ and only the harmonic component that is in phase with the modulation is required for measurement.

The achromatic half-wave plate is fabricated by laminating three separate, chromatic half-wave plates together, according to the strategy of Pancharatnam.[8] The instrument can access wavelengths in the range of 350–700 nm.

4. ELECTRIC FIELD-INDUCED ANISOTROPY IN DENSE COLLOID HARD-SPHERE SUSPENSIONS

The presence of a uniform electric field in a system of dielectric spheres suspended in a dielectric fluid will cause the spheres to aggregate in a fibrilated microstructure between the electrode pair. This reversible effect is due to polarization-induced dipole–dipole interactions and is the basis for numerous applications such as electrorheology and dielectrophoresis. Formation and breakdown of the fibrilated microstructure occurs on time scales of the order of tens of milliseconds and is completely reversible.

Electrorheology refers to the adjustment of fluid flow properties upon the application of an electric field. The fibrilated structure and increased length scales of the aggregates induced by the applied electric field result in both an enhanced fluid viscosity and a yield stress. This phenomena has led to many proposed electromechanical devices that rely on the ability to rapidly modify the rheological properties of a fluid. The force that moves particles together in a uniform field will cause them to translate in a non-uniform field. This polarization-induced translation of neutral particles is known as dielectrophoresis and is often used to separate and concentrate suspensions of particulates.

It is possible to visualize this aggregation process in a suspension if the

concentration of the spheres is not too large, and if Brownian motion does not blur the placement of the particles. However, to probe the structure and dynamics of particle motion in highly concentrated colloidal suspensions, alternative methods must be employed. For a suspension of hard spheres with no intrinsic optical anisotropy, dichroism will result only if the spatial arrangement of the spheres, as described by the pair distribution function, is anisotropic. Therefore, scattering dichroism, performed at variable wavelengths, will provide moments of the pair distribution as a function of the dimensionless wavenumber, where the dimensionless wavenumber is defined as $4ka$ with a the sphere radius and $k = 2\pi n/\lambda$.

Experimental System

To unambiguously measure the optical properties of concentrated media, the optical path length must be sufficiently small that multiple scattering is minimized. This can be accomplished by either reducing the thickness of the sample, as is done in the experiments on the polymer liquid crystals, or by matching the indices of refraction between the particles and the suspending fluid. It is also desirable to have a system of monodisperse spheres. These objectives can be achieved using silica particles, which can be synthesized with narrow size distributions and coated with short-chain hydrocarbons. These coatings allow the particles to be dispersed in a variety of organic solvents and protect the particles against aggregation. Detailed descriptions of the synthesis and coating procedures are found in refs. 9–11. Table I summarizes the particle sizes, coatings, and solvents that were used.

Electric Field Cell

The measurements were carried out using a stainless steel parallel plate electric field cell. The cell had a path length of 1.27 cm and the plates

Table I. Systems of Particle/Coating/Solvent Combinations[a]

System	Particle size	Particle coating	Solvent
1	150 nm	Octadecanol	Cyclohexane
2	214 nm	Octadecanol	Cyclohexane
3	460 nm	TPM/TMS	EtOH/toluene
4	700 nm	TPM/TMS	EtOH/toluene

[a] EtOh, ethanol; TPM, 3-methyacryloxypropyltrimethoxysilane; TMS, trimethyl silanol.

were spaced at 1 mm. Electric fields from 100 to 1000 V/mm have been used in this work. The light used in the dichroism measurements propagated parallel to the electrodes.

Experimental Results

Figure 2 shows the dichroism plotted as a function of time for a suspension of 150-nm particles at a volume fraction of 15%. Application of an electric field of 1000 V/mm at $t = 1$ causes an anisotropic structure in the sample; the result is an increase in the dichroism of the suspension. In an isotropic suspension of spheres, this can only arise from anisotropy in the spatial arrangement of their centers of mass. The effect is reversible and the dichroism relaxes to zero once the field is removed. The steady-state dichroism results are plotted in Fig. 3 against the square of the electric field for 150-nm particles at 15% volume fraction. Wavelengths from 350 to 750 nm are illustrated. At sufficiently low field strengths, the dichroism is linear in E^2, but as the field strength is increased, the dichroism tends to level out. This leveling out is not caused by a decrease in suspension anisotropy at higher field strengths, but rather reflects the sensitivity of the dichroism to the wavelength of light used for the measurement. This is further illustrated in Fig. 4.

In Fig. 4, the slope of the linear portion of the data in graphs similar to Fig. 3 is plotted against the dimensionless wavenumber. The dichroism

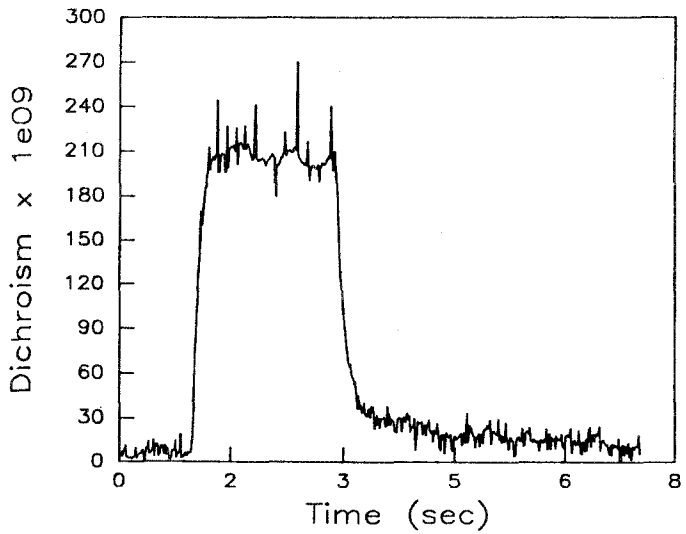

Fig. 2. The dichroism plotted as a function of time for a suspension of 150-nm particles at a volume fraction of 15%. Application of an electric field of 1000 V/mm at $t = 1$ sec.

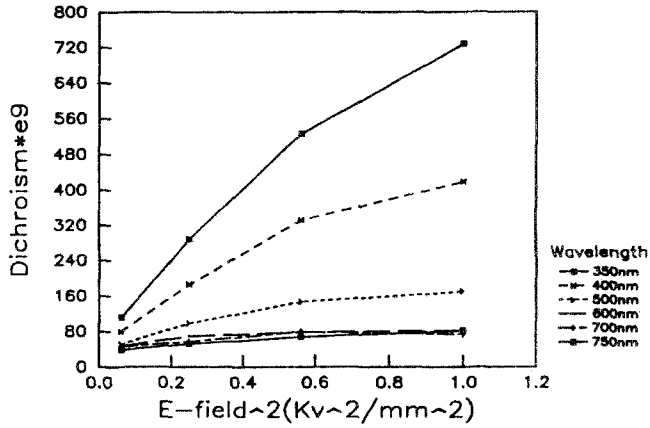

Fig. 3. The steady-state dichroism plotted against the square of the electric field for 150-nm particles at 15% volume fraction. Wavelengths from 350 to 750 nm are illustrated.

has been normalized by the suspension concentration, turbidity, and the particle volume. To cover such a range of wavenumbers requires particles of several sizes as given in Table I. The periodic behavior of the data is evidence of the sensitivity of the dichroism measurement to the ratio of the particle or aggregate size to the wavelength of light. Specifically, as the dimensioness wavenumber K is increased, the observed dichroism reflects anisotropy in structure over increasingly smaller length scales. Oscillations in the spatial position of the spheres that is described through the particle

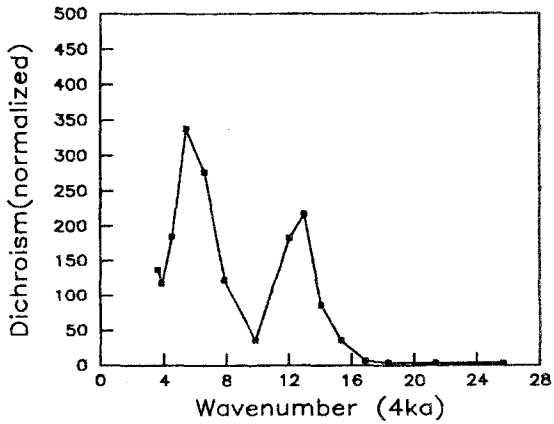

Fig. 4. The slope of the linear portion of the data in graphs similar to Fig. 3 plotted against the dimensionless wavenumber. The dichroism has been normalized by the suspension concentration, turbidity, and the particle volume. Data are illustrated for a volume fraction of 15%.

pair distribution function are directly reflected in the dichroism data. Data are illustrated for a volume fraction of 15%, but we have found similar oscillating behavior at other volume fractions.

Adriani and Gast[2] have developed statistical models to predict the dichroism of concentrated hard-sphere suspensions subject to electric fields. They model the electric field-induced fibrilation by considering the particle system to be hard spheres with aligned field-induced dipole moments.[12] These dipole moments cause clustering of the particles into an anisotropic suspension characterized by a particle pair distribution function. The dichroism of such a suspension is then calculated by considering the results of Onuki and Doi,[6] shown in Eq. (1). Theoretical calculations by Adriani show qualitative agreement with experimental results. Specifically, their results predict the linear increase and leveling out of the dichroism as the electric field is increased. They also predict the periodic behavior of the dichroism when plotted against the dimensionless wavenumber as illustrated in Fig. 4. The location of the first peak in the dichroism at $4ka = 12$ is predicted, as is the fact that the sign of the dichroism is positive. A detailed comparison of the experimental results with the theoretical predictions is the subject of a forthcoming publication.

5. DYNAMICS OF POLYMER LIQUID CRYSTALS

The flow response of polymer liquid crystals (PLCs) is markedly different from isotropic polymer liquids. This is manifested by such phenomena as negative, first normal stress differences[13] and highly oscillatory responses during transient flows.[14,15] Microstructural descriptions of these phenomena are made particularly difficult due to the complexity of structures that are present in PLCs. These anisotropic fluids are characterized by long-range order as a result of orientational and positional coupling of the macromolecules (usually rigid, rodlike in conformation). In its simplest form, this coupling results in nematic structure where the centers of mass are not correlated, but their orientations are predominantly along a single direction at any point in space. This is represented by a director field where the magnitude of this vector measures the degree of alignment. Simple nematics, or "single-domain" PLCs where the director changes continuously in space, are difficult to produce and defects are normally present in the form of line disclinations.

In the vicinity of such a defect, the director undergoes a discontinuous change in orientation. Depending on the geometry of the defect, gradients in the director will store elastic energy as a result of bending or splaying of the vector. The density of these defects will define a characteristic length scale a for the size of "domains." Recent electron micrographs of PLCs

indicate separation distances in the range of 1 μm for many systems.[4] These are regions containing a sufficient number of defects to envelope a volume of fluid having no net orientation. In other words, even though order exists at length scales on the order of the chains themselves, at larger length scales, the presence of defects diminishes this anisotropy.

Molecular models formulated to describe PLCs normally do not account for the presence of defects or elastic forces. The Doi model, for example, predicts the order parameter tensor for a defect-free, spatially homogeneous nematic subjected to flow.[16] Nonetheless, it is capable of predicting a number of nonlinear phenomena, such as a decreasing shear viscosity with increasing concentration, and negative first normal stress differences. This latter effect, explained recently by Marrucci and Maffettone,[17] is related to a phenomenon known as "director tumbling." Tumbling of the director field may be predicted by the earlier linear continuum Leslie–Ericksen model.[3] This theory models the liquid crystal through the director field $\mathbf{n}(\mathbf{r})$. This vector is subject to the following torque balance:

$$\mathbf{n} \times \left[\mathbf{h} - (a_6 - a_5)\mathbf{n} \cdot \mathbf{E} - (a_3 - a_2)\left(\frac{\partial \mathbf{n}}{\partial t} - \mathbf{n}\boldsymbol{\Omega} \right) \right] = 0 \tag{5}$$

where $\mathbf{h}$ is known as the "molecular field"[3] and $\mathbf{n} \times \mathbf{h}$ represents the torque due to spatial variations in the director field; thus, unlike the Doi model, the Leslie–Ericksen model can account for distortional elastic effects and inhomogeneity in the fluid structure. The remaining terms in this expression are hydrodynamic torques acting the director field, with $\mathbf{E}$ and $\boldsymbol{\Omega}$ the rate of strain and vorticity tensors, respectively. The phenomenological coefficients a_i have units of viscosity. Director tumbling is easily explained by considering only the hydrodynamic torques; neglecting elastic torques in the above expression leads to

$$\frac{\partial \mathbf{n}}{\partial t} - \mathbf{n}\boldsymbol{\Omega} - \lambda(\mathbf{n} \cdot \mathbf{E} - \mathbf{E} : \mathbf{nnn}) = 0 \tag{6}$$

Here $\lambda = -(a_6 - a_5)/(a_3 - a_2)$. When $\lambda < 1$, this expression is identical to the equation governing the dynamics of a rigid ellipsoid in a flow field (the Jeffery problem). Thus, in shear flow, when $\lambda < 1$, the hydrodynamic torques always act to rotate the director in a periodic orbit. This expression may be reproduced by taking the linear limit of the Doi model. It has been shown that the rigorous Doi model does in fact predict director tumbling in the linear limit.[18]

Experimentally, it has not yet been conclusively demonstrated whether

PLC solutions exhibit tumbling. Experiments by Berry and Srinivasarao on a defect-free solution of PBT are somewhat ambiguous about whether tumbling occurs (see their paper in this issue). Liquid crystalline solutions of polypeptides exhibit behavior, such as negative first normal stress differences and strong oscillatory responses in transient flows, that is strongly consistent with the prediction of tumbling. Here we will focus on oscillatory responses.

Mewis and Moldenaers[14] have observed that the shear stress exhibits a pronounced oscillatory response in transient shear flows. These oscillations scale with shear strain, in accord with the predictions of Eq. (6) for tumbling systems. During flow it is expected that the many defect structures in PLCs will become oriented, resulting in a linear dichroism that can be observed as a means of probing the structural response of the PLC directly. Figure 5 shows the optical results of a flow reversal experiment on a liquid crystalline solution of a polybenzylglutamate. Accompanying the initiation of shear flow is an irreproducible oscillatory response that reflects the structural indeterminacy of a textured sample at rest. Following 200 strain units, the flow is reversed, and a set of oscillations is clearly observed. Unlike the oscillations at flow inception, these oscillations are completely reproducible, indicating that pre-shearing creates a useful initial condition for studying the dynamics of these systems. After 200 strain units in the

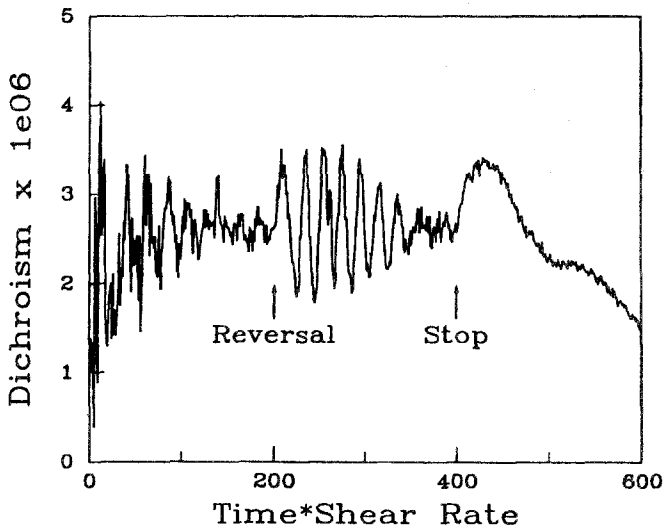

Fig. 5. Dichroism plotted against time for a flow reversal experiment on a liquid crystalline solution of polybenzyl-*l*-glutamate at 12% in *m*-cresol. Following 200 strain units, a shear flow of 0.75/sec is reversed. After 200 strain units in the reverse direction, the flow is stopped. A wavelength of 500 nm was used.

reverse direction, the flow is stopped, and the dichroism relaxes in a complicated and irreproducible manner.

Repeating this experiment at different shear rates shows that the oscillations in structure scale with shear strain; thus, it is quite clear that the observed response in the shear stress reflects an oscillatory transient change in the PLC structure. By performing the dichroism measurement at various wavelengths, different length scales of the complicated PLC structure may be probed. It is observed that over the entire range of wavelengths accessible to the instrument, the oscillations occur with exactly the same period of shear strain. This is again consistent with the prediction of the Doi model that the tumbling period is a material parameter, and hence there should be only one characteristic period of oscillation, regardless of the length scale of the observation.

A serious shortcoming of the Doi model is that there is no way to account for spatial inhomogeneity of the director field and associated elastic torques. For tumbling systems, elastic torques due to boundary-induced orientation have a substantial effect on the predicted dynamics. Although Eq. (6) predicts an oscillatory response that would persist indefinitely in shear flow, the inclusion of boundary-induced elastic torques as in Eq. (5) limits the extent to which the director may rotate, and ultimately leads to a steady state.

An example of a shear flow reversal calculation for a tumbling nematic based on the full Leslie–Ericksen model is presented in Fig. 6. In this calculation, the director is assumed to be anchored perpendicular to the two boundaries defining the shear flow. The material parameters are chosen for the low-molecular-weight nematic 8CB, kown to exhibit tumbling at 35°C.[19] The two variables plotted are θ_m, the maximum degree of director rotation away from its initial boundary-induced orientation, and the dimensionless shear stress. Upon inception of shear flow, the director begins to rotate under the influence of hydrodynamic torques. However, since the director is anchored at the wall, elastic torques arise that tend to oppose the continued rotation of the director, so that eventually the director rotation stops, and a steady state is reached. The critical parameter in these calculations is the Ericksen number Er, representing a ratio of hydrodynamic to elastic torques:

$$Er = \frac{|a_2|\,\dot{\gamma} d^2}{K_1} \tag{7}$$

where $\dot{\gamma}$ is the macroscopically applied shear rate, d is the distance between the plates, and K_1 is the splay elastic constant. For the moderately large value of Er used in Fig. 6, the hydrodynamic torques are sufficiently strong

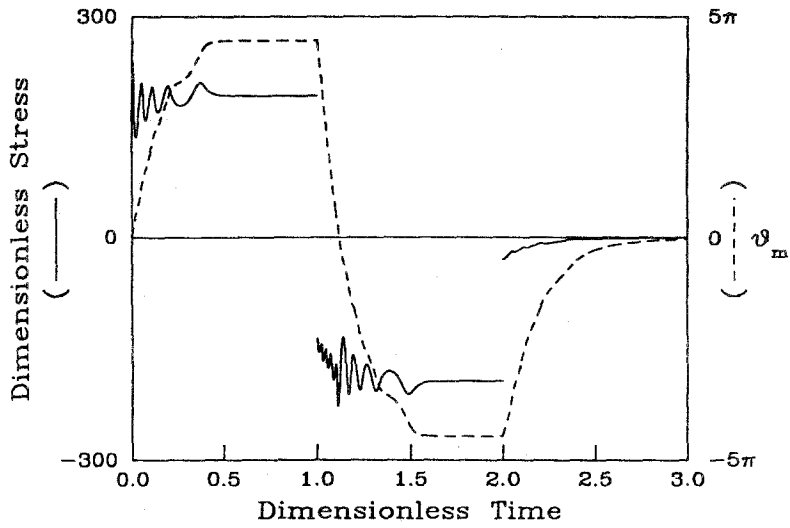

Fig. 6. Plot of θ_m, the maximum degree of director rotation, and the dimensionless shear stress against strain for a flow reversal experiment predicted using the Leslie–Ericksen model. The material parameters are chosen for the low-molecular-weight nematic 8CB.[19] The parameter in these calculations is the Ericksen number *Er*.

to rotate the director through several multiples of π before the elastic torques frustrate continued rotation. While the director "winds up," the viscous resistance of the fluid changes in consequence of its changing structure, so that the shear stress is seen to exhibit an oscillatory response, similar to that observed by Moldenaers and Mewis.

When the direction of flow is changed, the hydrodynamic and elastic torques briefly act together to rotate the director first back toward its initial condition, after which a response quite similar to the initial transient is seen. Oscillatory behavior in transient shear flows of liquid crystals may therefore be straightforward manifestations of director tumbling. When the flow is stopped, the director field relaxes back to its initial condition under the influence of elastic forces. The rotation of the director produces a stress relaxation phenomenon. In addition, although there is no net flow, the relaxing director profile does drive a secondary flow during relaxation.[20] Despite the simplicity of the Leslie–Ericksen model, a wide variety of unusual phenomena are predicted in even this simple flow field.

The calculations in Fig. 6 are in a highly idealized geometry. However, it is possible that the important physical ideas may apply to a textured polymer, if one assumes that defects act in some way as constraints on the director field, similar to strong anchoring at a boundary. In this case, the

appropriate length scale for calculating the Ericksen number would be some average distance between defects. When this approach is taken, the essential features of many other observations, such as large constrained recoils and certain relaxation scaling laws, may be rationalized based on such idealized calculations.[20]

6. CONCLUSIONS

Measurement of scattering dichroism has been demonstrated to probe the long-range microstructure of two complex fluids comprised of rigid elements. In the case of electric field-induced structure in dense suspensions of spheres, measurement of this quantity provides a direct measure of a moment of the Fourier transform of the particle pair distribution function. In this case, it is particularly valuable to make this measurement as a function of the ratio of the length scale of the scattering spheres to the wavelength of light. This measurement picks up an oscillatory structure that reflects the oscillatory nature of the pair distribution function. Although not shown here, the magnitudes of the peaks shown in Fig. 4 are a strong function of the volume fraction of the spheres and are strongly damped as the volume fraction is increased. This is a consequence of the fact that it is easier to create high-aspect-ratio aggregates with spheres set in well-defined spatial positions at lower volume fractions. At higher concentrations, there is a greater tendency for the spheres to cluster in highly branched groups.

The use of scattering dichroism in the study of polymer liquid crystals offers a method of examining structure at a length scale comparable to the defect structure in these liquids. This is important, since anisotropy also exists at the length scale of the polymer chains themselves. Birefringence, the anisotropy in the real part of the refractive index tensor, cannot be used to make a separation in the dynamics of anisotropic structure at these two length scales, but scattering dichroism can. This is because the dichroism only arises from polarization scattering by the defects and is not affected directly by the presence of local ordering of the chains. The experiments measuring dichroism from a polymer liquid crystal subject to transient shear flow reveal a highly oscillatory response that is reminiscent of the predictions of the Leslie–Ericksen model when elastic restoring forces are included in the calculation.

ACKNOWLEDGMENTS

We thank N. J. Wagner for his assistance in the preparation of the monosized, colloidal spheres. The portion of the work involving suspen-

sions subject to electric fields was sponsored by a grant from the National Science Foundation (CBT 8814236). The research into the dynamics of polymer liquid crystals was supported by a grant from the Petroleum Research Fund of the ACS (ACS/PRF 18218).

REFERENCES

1. N. Wagner, G. Fuller, and W. Russel, *J. Chem. Phys.* **89**:1580 (1988).
2. P. Adriani and A. Gast, Predictions of birefringence and dichroism of hard sphere suspensions in combined shear and electric fields, *J. Chem. Phys.*, submitted.
3. P. G. de Gennes, *The Physics of Liquid Crystals* (Clarendon Press, Oxford, 1974).
4. B. A. Wood and E. L. Thomas, *Nature* **324**:655 (1986).
5. G. G. Fuller, *Annu. Rev. Fluid Mech.* **22**:387 (1990).
6. A. Onuki and M. Doi, *J. Chem. Phys.* **85**:1190 (1986).
7. G. G. Fuller and K. J. Mikkelsen, *J. Rheol.* **33**:761 (1989).
8. S. Pancharatnam, *Proc. Ind. Acad. Sci. A* **41**:130 (1955).
9. A. Philipse, Ph.D. Thesis, de Rijksuniversiteit te Utrecht (1987).
10. N. J. Wagner, Ph.D. Thesis, Princeton University (1989).
11. N. J. Wagner and W. B. Russel, *Phys. Fluids* (April 1990).
12. J. Hayter and R. Pynn, *Phys. Rev. Lett.* **49**:1103 (1983).
13. G. Kiss and R. S. Porter, *J. Polym. Sci.: Phys.* **18**:361 (1980).
14. J. Mewis and P. Moldenaers, *Mol. Cryst. Liq. Cryst.* **153**:291 (1987).
15. P. Moldenaers, G. Fuller, and J. Mewis, *Macromolecules* **22**:960 (1989).
16. M. Doi and S. F. Edwards, *The Theory of Polymer Dynamics* (Clarendon Press, Oxford, 1986).
17. G. Marrucci and P. L. Maffettone, *Macromolecules* **22**:4076 (1989).
18. N. Kuzuu and M. Doi, *J. Phys. Soc. Japan* **53**:1031 (1984).
19. T. Carlsson, *Mol. Cryst. Liq. Cryst.* **104**:307 (1984).
20. W. R. Burghardt and G. G. Fuller, *J. Rheol.*, submitted.